UNIVERSITÀ DEGLI STUDI DI TORINO

Dario Livio Longo, Juan Carlos Cutrin, Filippo Michelotti, Pietro Irrera, and Silvio Aime

Noninvasive evaluation of renal pH homeostasis after ischemia reperfusion injury by CEST-MRI

In NMR IN BIOMEDICINE 2017, 30, e3720

DOI: 10.1002/nbm.3720

Title

Noninvasive evaluation of renal pH homeostasis after ischemia-reperfusion injury by CEST-MRI

Authors

Dario Livio Longo, PhD[1,2], Juan Carlos Cutrin, PhD[2], Filippo Michelotti, MSc[2], Pietro Irrera, MSc[2] and Silvio Aime, PhD[2]

[1] Istituto di Biostrutture e Bioimmagini (CNR) c/o Centro di Biotecnologie Molecolari, Torino, Italy

[2] Dipartimento di Biotecnologie Biomolecolari e Scienze per la Salute, Università degli Studi di Torino, 10126, Torino, Italy

Corresponding Author

Dario Livio Longo, Istituto di Biostrutture e Bioimmagini (CNR) c/o Centro di Biotecnologie Molecolari, Via Nizza 52, 10126, Torino, Italy

Phone: +39-011-6706473, Fax: +39-011-6706487, email: dario.longo@unito.it

Running Title

MRI-CEST pH mapping of acute kidney injury

Keywords

acute kidney injury, ischemia reperfusion injury, MRI, CEST, pH homeostasis

word count: 5156

ABBREVIATION USED

AKI	acute kidney injury
ATN	acute tubular necrosis
KIRI	kidney ischemia-reperfusion inury
sCr	serum creatinine
BUN	blood urea nitrogen
CEST	chemical exchange saturation transfer
ROI	Region ff interest
H&E	hematoxylin and eosin

Abstract

Acute kidney injury (AKI) in mice caused by sustained ischemia followed by reperfusion is associated with acute tubular necrosis and renal dysfunctional blood flow. Despite the principal role of the kidney is the maintenance of acid-base balance, current imaging approaches are unable to assess this important parameter and clinical biomarkers are not robust enough in evaluating the severity of kidney damage. Therefore, novel noninvasive imaging approaches are needed to assess *in vivo* the acid-base homeostasis. This study investigates the usefulness of magnetic resonance imaging (MRI) - chemical exchange saturation transfer (CEST) pH imaging in characterizing moderate and severe AKI in mice following unilateral ischemia-reperfusion injury. Moderate ischemia (20 min) and severe ischemia (40 min) were induced in Balb/C mice that were imaged at 4 time points thereafter (days 0, 1, 2, 7). A significant increase of renal pH values was observed as early as one day after the ischemia-reperfusion damage for both moderate and severe ischemia. MRI-CEST pH imaging distinguished the evolution of moderate from severe AKI. A recovery of normal renal pH values was observed for moderate AKI, whereas a persisting renal pH increase was observed for severe AKI at day 7. Renal filtration fraction was significantly lower for clamped kidneys following impairment of glomerular filtration. Notably, renal pH values were significantly correlated with the histopathological score. In conclusion, MRI-CEST pH mapping is a valid tool for the noninvasive evaluation of both acid-base balance and renal filtration in patients with ischemia-reperfusion injury.

INTRODUCTION

Ischemic renal injury is a severe clinical problem in nephrology and the major cause of acute kidney injury (AKI).[1] Hospitalized patients commonly experience AKI that is strongly associated with poor prognosis and high mortality.[2] Moreover, patients may develop a progressive renal dysfunction even with initial recovery of renal function.[3] Despite advances in clinical care and therapeutic interventions, morbidity and mortality remain high, largely due to the incomplete understanding of AKI pathophysiology and to the limitation of currently techniques for diagnosis. In fact, conventional biomarkers such as blood urea nitrogen (BUN) and serum creatinine (sCr) are unable to fulfil diagnostic criteria.[4] BUN production is inconstant and can be altered by non renal factors, whereas sCr values become pathological if more than half of the glomerular filtration rate is lost. In addition, increases in blood concentrations become detectable only 24 hours after the occurrence of the pathological event.[5] Therefore, the noninvasive evaluation and monitoring of renal function may allow a timely and definitive diagnosis of AKI.

Functional magnetic resonance imaging (MRI) provides several approaches, such as diffusion-weighted imaging,[6] blood oxygen level dependent imaging,[7] arterial spin labelling,[8] longitudinal and transverse relaxation time measurements,[9, 10] dynamic contrast enhanced imaging,[11] hyperpolarized magnetic resonances spectroscopy,[12] and sodium MRI,[13] to assess renal function and pathophysiology beside anatomical information. All these MRI-based methods may be useful to determine renal pathology by quantification of renal water diffusion, oxygenation, perfusion, tissue water content and viability.[14-16]

In the context of the different physiological parameters that one may image *in vivo*, renal pH appears of outmost relevance, since the kidneys hold the key role of regulating the acid-base balance. In fact, survival of animals is heavily dependent on the acid-base homeostasis, since changes in pH could have marked outcomes on biological processes at several levels (cellular, tissue and whole animal). As a consequence, the rapid decline in kidney function following AKI will result in derangements in acid-base homeostasis.[17] Thus, imaging techniques able to report *in vivo* accurate pH measurements and longitudinal pH alterations would have a great clinical relevance not only for early identification of AKI but also for providing reliable predictions for further outcomes.

In recent years, the development of responsive MRI contrast agents that report on tissue pH have attracted considerable attention, owing to the altered production of acids that occur in several pathologies.[18] Chemical exchange saturation transfer (CEST) is a novel MRI approach in which the contrast is generated by saturating specific exchangeable protons on either endogenous or exogenous molecules.[19, 20] Owing to the sensitivity of the proton exchange rate to a variety of chemical and physical factors, including pH, several CEST pH-responsive probes have been demonstrated to measure tissue pH.[21-28] Among them, iopamidol is a clinical approved radiographic agent that was demonstrated to report accurate renal pH values, independently from the concentration, both at preclinical and clinical levels.[21, 29] Notably, altered renal pH values have been observed in a glycerol-induced murine model of ATN involving both kidneys by exploiting MRI-CEST pH mapping with iopamidol.[30]

Considering that ischemia is the main aetiology in human AKI, and that pH may represent a good biomarker for its detection, it was deemed of interest whether MRI-CEST renal pH mapping can detect early renal damage and distinguish AKI recovery from irreversible damage in a unilateral kidney ischemia reperfusion injury (KIRI) model. The unilateral ischemia reperfusion injury model was used because of the advantage that only one kidney is damaged, whereas the contralateral kidney is not affected. Consequently, in this model of post-ischemic AKI, serum biomarkers are minimally affected, since the contralateral kidney can compensate for the reduced renal functionality. Moreover, as the entity of the damage is dependent on the time of ischemia, this model appears suitable to fairly reproducing different human conditions of post-ischemic damage evolution, since some patients may spontaneously recuperate normal renal functionality after few days, whereas for others the initial insult did not resolve and progressively evolves to the end-stage kidney disease.[31] The aim of this study was to assess if MRI-CEST pH mapping can detect the early onset of acute kidney damage and distinguish between the recovery and persistence of the damage following unilateral ischemia reperfusion injury in mice.

METHODS

Animal model

BALB/c mice were purchased from Charles River Laboratories (Calco, Italy) and maintained in specific pathogen-free conditions. All animal experiments were approved by the University Ethical Committee and performed in accordance with the European guidelines under directive 2010/63. The model of normothermic unilateral renal ischemia reperfusion injury was performed as follows. Briefly, after anaesthesia with a mixture of tiletamine/zolazepam 20 mg/kg (Zoletil 100; Virbac, Milan, Italy) and 5 mg/kg xylazine (Rompun; Bayer, Milan, Italy) injected intramuscular, mice were submited to a midline laparatomy to expose the left renale pedicle, then it was occluded with a vascular clamp for 20 min (n=14 mice) or 40 min (n=15 mice). For longitudinal MRI-examinations, n=6 animal with moderate AKI and n=7 animals with severe AKI were used. Some on the animals were killed on day1 (n=4 with 20 and 40 min KIRI) and on day 7 (n=4 with 20 and 40 min KIRI) for histology work up. Sham operation was performed on the right vascular pedicle for comparison (n=6 mice). Interventions were performed under a thermic lamp to maintain constant the mice body temperature. At the end of the ischemic injury mice were allowed to recovery and supplemented with 1 ml of sterile 0.9% NaCl solution administered subcutaneously. Animals were examined by MRI before and 1, 2 and 7 days after renal re-flow.

In vivo magnetic resonance imaging studies

Chemical exchange saturation transfer pH imaging

MRI images were acquired with a 7T MRI micro-imaging vertical scanner (Avance 300, Bruker Biospin, Germany). A 30 mm birdcage resonator was used for both transmission and receiving. During imaging, each mouse was anesthetized by injecting a mixture of tiletamine/zolazepam 20 mg/kg (Zoletil 100; Virbac, Milan, Italy) and 5 mg/kg xylazine (Rompun; Bayer, Milan, Italy). Respiratory rate was continuously monitored using a respiratory air pillow (SA Instruments, Stony Brook, NY; USA).

Kidneys were localized with axial and coronal T_2-weighted images covering the whole kidneys. A high spatial resolution T_2-weighted image (field of view of 3x3 cm, matrix of 256x256, slice thickness of 1.5mm, in-plane resolution of 117 µm) was acquired for placing the region of interests (ROI) for correct delineation of the whole kidney. A single-shot RARE sequence (TR = 6s, TE = 4.1ms, Rare Factor = 96, centric

encoding = 1) preceded by a 3μT cw presaturation pulse for 5 s and by a fat-suppression module was used to acquire Z-spectra. The CEST spectrum was acquired in the frequency offset range ±10 ppm with 37 offsets unevenly separated. An acquisition matrix of 96x96 was reconstructed to 128x128 with a field of view of 3x3 cm (in-plane spatial resolution = 234 μm) and a slice thickness of 1.5 mm. The acquisition time for a single MR-CEST spectrum was ca. 4 min. MR-CEST images were acquired before and after i.v. injection of iopamidol (dose = 1.0 g iodine / kg body weight).

CEST analysis

All CEST images were analyzed using a Matlab-based home-made script (The Mathworks, Inc., Natick, MA, USA). The Z-spectra were interpolated by cubic splines, B_0-shift corrected and saturation transfer efficiency (ST%) was measured by punctual analysis . A threshold value of 2% was set, based on the ΔST variations between multiple pre-contrast ST maps (ca. 1.2% at 4.3 - 4.4 ppm) to discriminate between enhancing and not-enhancing pixels. pH values were estimated *in vivo* by applying the ratiometric approach on manually-defined region of interests.[21] The renal pH parametric maps were superimposed onto the anatomical reference image. Filtration fraction was calculated as the percent of detected pixels within the kidney region.

Histology and Renal Function

Following the completion of MRI experiments, mice were euthanized and kidneys were removed immediately for histological analysis. Sagittal sections of both kidneys were overnight fixed in 4% buffered formaldehyde solution. One experienced pathologist (JCC with more than 20 years of experience) evaluated the extent of renal damage as it was previously reported.[32] Histological examination were performed on de-waxed 5 μm PAS stained sections to evaluate the following parameters of tubular cell injury: loss of brush border (partial or complete loss of the brush border), vacuolar degeneration (presence of more than three cells with cytoplasmic vacuoles or blebs formation protruding into the lumen of the tubules), tubular dilatation (dilatation was considered when the tubular lumen was increased at least 20% versus normal co-respective), cell detachment (presence of necrotic or morphological well preserved isolated cells in the

tubular lumen), necrosis (presence of three or more cells with signs of coagulative necrosis, such as loss of cell boundaries with marked eosinophilia or extreme swelling together with nuclear changes consisting in pyknosis or chromatolysis or karyorrhexis), and formation of casts (presence of granule-hyaline, mucous or proteinaceous material in the tubular lumen). Five non consecutive fields from the cortex and the outer medulla were evaluated (magnification 200x). Renal injury scores were determined by the percentage of tubules involved: 0 = 0; 1 = up to 10%; 2 = 11–20%; 3 = 21–40%; 4 = 41–60%; 5 = more than 61%. Overall histological score was obtained by summing all the individual parameters of injury.

Blood was collected to measure serum creatinine (sCr) and blood urea nitrogen (BUN) levels in SHAM and KIRI groups at different time points. In addition, urinary pH values were measured by collecting urine just after the MRI experiments.

Statistical analysis

Renal pH values were measured before and after ischemic reperfusion injury for both kidneys in each group. All values were expressed as mean ±SD unless otherwise stated. Analysis of variance (ANOVA) and Bonferroni's multiple comparison test was employed to compare the differences between groups. The Pearson product moment correlation test was used to search for correlation between parameters. A value of $P < 0.05$ was considered statistically significant. The statistical analysis was performed by using the GraphPad Prism 5 program package (GraphPad Inc, San Diego, California, USA).

RESULTS

Histological findings confirm reversible and irreversible renal damage

Histological evaluation confirmed extensive injury in the clamped kidneys as soon as 1 day after the induced ischemia, whereas in the contralateral ones a negligible damage was observed (Figure 1A). Anyway, different morphological pattern of damage was observed after 20 and 40 min of ischemia. At one day of re-flow upon 40 min of ischemia, kidneys showed severe morphological alterations in comparison with the

kidneys undergone to 20 min of ischemia (Figure 1B). Most of the proximal convoluted tubules throughout the major part of the outer medulla, exhibited a higher score of ATN consisting in loss of brush borders, tubular dilatation, cast deposition, cell detachment and tubular necrosis, in contrast to kidneys submitted to 20 min of ischemia (Figure S1). Even seven days after I/R injury, still high scores of tubular damage was observed for the 40 min clamped kidneys, whereas the 20 min ischemic injured kidneys showed practically a full recovery of the normal morphology. In view of these results, we like to propose herein this model of AKI as a well-defined condition of renal reversible and irreversible injury that can be followed by non-invasive imaging approaches to assess single kidney loss of morphology and functionality.

Serum biomarkers are not able to detect acute renal damage

There were no major differences between sCr levels before and after 20 min of ischemia/reperfusion injury in all animals (Figure 2A). There were no significant differences also for the BUN levels for the 20 min KIRI group (Figure 2B). This may be attributable to the well-functioning contralateral kidney and to the reduced damage in the clamped one, that overall indicates an unsuitability of serum biomarkers to assess the natural progression of mild renal damage upon ischemia/reperfusion injury. The 40 min KIRI group showed a moderate increase in both sCr and BUN levels at both one and seven days following reperfusion injury, with statistically significance only after 7 days for the BUN levels (31.4 ±3.0 vs 19.9 ±2.2, $P<0.01$, for KIRI and SHAM groups, respectively).

Urine pH values between animals with moderate AKI and SHAM were not significantly different at both day 1 and day 7 (Figure 2C). In the acute phase, at day 1 after severe AKI injury, urine pH values were higher than the sham group (pH=5.8 ±0.3 vs 5.0 ±0.5). In contrast to the moderate AKI group, at day 7 after surgery urine pH values in the severe AKI group were still increased. These results confirm the inability of current biomarkers to assess the early onset of single kidney damage.

CEST pH detects KIRI acute damage and recovery upon 20 min ischemia injury

After moderate AKI, MRI-CEST pH mapping detected elevation of renal pH values in the clamped kidney indicating renal damage that was most pronounced at 1 day and 2 days post ischemia (Figure 3A). pH values were significantly higher at day 1 (pH=7.0 ±0.2, P<0.01) and at day 2 (pH=6.9 ±0.2, P<0.01) compared to baseline (pH=6.7 ±0.2) for clamped kidneys. A significant increase of the pH values was observed in comparison to contralateral control kidneys without AKI at day 1 (6.7 ±0.2 vs 7.0 ±0.2, P<0.05). No significant changes of pH values were observed in the contralateral kidney without AKI compared with baseline. Examples of T_{2w} anatomical images and corresponding pH maps at different time points after the moderate AKI are given in Figure 4A and 4B.

CEST pH detects KIRI acute and persistent damage upon 40 min ischemia injury

The pH values were increased after the severe AKI onset at day 1, with more conspicuous variations at day 2 (Figure 3B). At day 1, the pH values increased to 7.0 ±0.1 in comparison to baseline values (6.7 ±0.2, P<0.01) and peaked at day 2 (pH=7.0 ±0.1, P<0.01). In contrast to moderate AKI, the pH values remained significantly elevated until day 7 (pH=6.9 ±0.2, P<0.01). A significant difference between the moderate and severe AKI was observed at this time point (P<0.01). In the contralateral kidney without AKI, pH values were unchanged throughout the entire observation period with a slight increase of pH values at day1. Examples of T_{2w} anatomical images and pH maps of one animal with severe AKI are shown in Figure 4C and 4D.

CEST renal filtration fraction distinguishes between kidney damage recover and progression

Since the pH-responsive contrast agent is completely excreted by kidneys, with no secretion or reabsorption, its detection in renal compartments can be considered an indirect measurement of renal filtration and changes in detection may reflect alterations in the glomerular filtration. Significant impairment of renal filtration measured by means of the filtration fraction estimate compared with values before surgery was detectable since 1 day after moderate and severe AKI (Figure 5). For animals with moderate AKI, filtration fraction of clamped kidney (0.56 ±0.21) was found to be significantly lower (P<0.01) than that of contralateral kidney

(0.84 ±0.16) at 1 day after injury. After moderate AKI, renal filtration nearly returned to baseline by day 7. After severe AKI, filtration impairment of clamped kidneys persisted until day 7 (0.57 ±0.05, 0.52 ±0.11 and 0.38 ±0.12 after 1, 2 and 7 days, respectively; $P<0.01$).

Correlation of renal pH values with histological damage

MRI-CEST derived pH values significantly correlated with histological scores ($r=0.87$, $P<0.01$; Figure 3C).

DISCUSSION

The herein reported results show, for the first time, that MRI-CEST pH mapping allows the noninvasive detection and monitoring of renal function impairment after unilateral ischemia-induced AKI. The derangement of pH regulation was correlated to the decay of renal filtration function and to the severity of the morphological damage.

In this study, CEST pH imaging revealed significantly higher renal pH values indicating renal function impairment, in the clamped kidneys compared with the control ones, even after 1 day, independently of the duration of the ischemic injury. At this time point serum biomarkers were unable to detect renal damage and, based on AKIN criteria,[33] animals could not be classified as having AKI. On the other hand, histopathological damages at this time point were minor for the moderate AKI, with limited cast deposition and tubular dilatation (Figure S1). Therefore, our data would suggest that MRI-CEST pH mapping can be a promising tool for assessing single kidney injury and severity of AKI.

We already established and validated the MRI-CEST pH mapping methodology for assessing AKI in mice induced by glycerol injection.[30] Here, the unilateral model was chosen without nephrectomy since the renal function of the contralateral kidney is not compromised, leading to a milder and minimally invasive damage to identify physiological changes earlier than elevation of serum creatinine. In addition, the contralateral non-ischemic kidney may be used as a self-internal control for each animal due to the absence of functional and morphological damages. Furthermore, ischemia times of 20 and 40 min result in different kidney time

course damage evolution, with shorter times that allows for recovery, whereas prolonged ischemia times evolve in end-stage kidney disease.[34, 35]

In this study, renal pH-values of the injured kidney significantly increased after AKI relative to the contralateral one, at both the ischemia times. This might be related to the impaired regulation of acid-base balance. In fact, the systemic HCO_3^- concentration is regulated by kidneys through the absorption of all the filtered HCO_3^- and the production of new HCO_3^- to replace that consumed by non-volatile acids upon protein metabolism .[17] The production of new HCO_3^- is actually done by net acid excretion. It follows that with the reduction in number of functioning nephrons, the capacity of the kidney to excrete acids into urine or reabsorb bicarbonate is compromised, hence resulting in an increase of renal pH values. In addition, elevated renal pH values occurred just 1 day after AKI and persisted until 1 week in the the severe AKI model. Moreover, renal pH evolution significantly correlated with histopathologic-based scores, with a recovery of the renal damage after 7 days for the moderately injured kidneys, whereas a persistent damage was observed for the prolonged ischemia time (40 min). Therefore, MRI-CEST pH mapping allowed the distinction of moderate from severe AKI.

Considering that functional renal impairment often precedes anatomical changes, imaging modalities are of interest owing to their capability of non-invasive and longitudinal assessment of renal function. Early functional changes have previously been investigated in several models of ischemia-reperfusion AKI following the administration of Gd-based contrast agents. Most of these studies addressed the quantification of renal perfusion and estimation of glomerular filtration rate both at preclinical and clinical levels.[6, 36-39] DCE-MRI methods are less time-consuming and costly than methods based on the clearance of injected tracers, and do not involve radiation issues, as in radionuclide renography.[40] All these methods exploit the reduced filtration function and changes in renal microvasculature to report on the ischemia reperfusion damage. Here we exploited a FDA-approved radiographic contrast agent that, sharing similar size and distribution/elimination properties with Gd-based extracellular fluid agents, allows indirect detection of reduced renal function. In fact, as a consequence of the decreased glomerular ability to filter the injected contrast agents, a marked decrease in the filtration fraction estimate was observed following the damage. Despite this simple estimate does not provide information on glomerular filtration rate or on renal blood

flow, it was found to be correlated with the severity and with the evolution of the kidney damage. In addition, proof-of-concept studies have demonstrated that iopamidol and other radiographic agents can also provide perfusion estimates.[41, 42]

Nevertheless, a major limitation of all these approaches relies in the assessment of only one function of the kidneys that is their filtration capability, while the balance of the acid-base homeostasis has never been addressed. It is important to recognize that disordered acid-base homeostasis contributes to the progression of chronic kidney disease and to increased morbidity and mortality in dialyzed patients.[43] Interestingly, chronic kidney disease progression can be tempered throughout normalization of acid–base homeostasis.[44] It follows that the CEST-pH mapping approach may play a fundamental role in assessing pH changes in kidney-related pathologies and in monitoring treatment response. Notably, the combined evaluation of two main factors that report on renal dysfunction, i.e. filtration fraction and renal pH values, is feasible only within this approach.

A limitation of this study was the reduced kidney coverage by acquiring only the central slice. However, also MRI-based measurements of glomerular filtration rate are commonly acquired in few representative slices. Several approaches for increasing volume coverage within the MRI-CEST acquisition have been recently proposed.[45, 46]

To conclude, we have demonstrated that MRI-CEST pH mapping can be a novel promising biomarker for diagnosis and monitoring of renal function, allowing an early detection of the occurrence of renal pathology and to distinguish moderate or severe AKI.

ACKNOWLEDGEMENTS

Cooperation agreement between IBB-CNR and Bracco Imaging SpA is gratefully acknowledged.

REFERENCES

1. Ali T, Khan I, Simpson W, Prescott G, Townend J, Smith W, Macleod A. Incidence and outcomes in acute kidney injury: a comprehensive population-based study. *J. Am. Soc. Nephrol.* 2007;18:1292-1298.

2. Wang HE, Muntner P, Chertow GM, Warnock DG. Acute kidney injury and mortality in hospitalized patients. *Am. J. Nephrol.* 2012;35:349-355.

3. Jones J, Holmen J, De Graauw J, Jovanovich A, Thornton S, Chonchol M. Association of complete recovery from acute kidney injury with incident CKD stage 3 and all-cause mortality. *Am. J. Kidney Dis.* 2012;60:402-408.

4. Ympa YP, Sakr Y, Reinhart K, Vincent JL. Has mortality from acute renal failure decreased? A systematic review of the literature. *Am. J. Med.* 2005;118:827-832.

5. Uchino S. Creatinine. *Curr Opin Crit Care.* 2010;16:562-567.

6. Oostendorp M, de Vries EE, Slenter JM, Peutz-Kootstra CJ, Snoeijs MG, Post MJ, van Heurn LW, Backes WH. MRI of renal oxygenation and function after normothermic ischemia-reperfusion injury. *NMR Biomed.* 2011;24:194-200.

7. Neugarten J, Golestaneh L. Blood oxygenation level-dependent MRI for assessment of renal oxygenation. *Int J Nephrol Renovasc Dis.* 2014;7:421-435.

8. Hueper K, Gutberlet M, Rong S, Hartung D, Mengel M, Lu X, Haller H, Wacker F, Meier M, Gueler F. Acute kidney injury: arterial spin labeling to monitor renal perfusion impairment in mice-comparison with histopathologic results and renal function. *Radiology.* 2014;270:117-124.

9. Hueper K, Peperhove M, Rong S, Gerstenberg J, Mengel M, Meier M, Gutberlet M, Tewes S, Barrmeyer A, Chen R, Haller H, Wacker F, Hartung D, Gueler F. T1-mapping for assessment of ischemia-induced acute kidney injury and prediction of chronic kidney disease in mice. *Eur. Radiol.* 2014;24:2252-2260.

10. Hueper K, Rong S, Gutberlet M, Hartung D, Mengel M, Lu X, Haller H, Wacker F, Meier M, Gueler F. T2 relaxation time and apparent diffusion coefficient for noninvasive assessment of renal pathology after acute kidney injury in mice: comparison with histopathology. *Invest. Radiol.* 2013;48:834-842.

11. Grenier N, Pedersen M, Hauger O. Contrast agents for functional and cellular MRI of the kidney. *Eur. J. Radiol.* 2006;60:341-352.

12. Clatworthy MR, Kettunen MI, Hu DE, Mathews RJ, Witney TH, Kennedy BW, Bohndiek SE, Gallagher FA, Jarvis LB, Smith KG, Brindle KM. Magnetic resonance imaging with hyperpolarized [1,4-(13)C2]fumarate allows detection of early renal acute tubular necrosis. *Proc. Natl. Acad. Sci. U. S. A.* 2012;109:13374-13379.

13. Zollner FG, Konstandin S, Lommen J, Budjan J, Schoenberg SO, Schad LR, Haneder S. Quantitative sodium MRI of kidney. *NMR Biomed.* 2016;29:197-205.

14. Notohamiprodjo M, Reiser MF, Sourbron SP. Diffusion and perfusion of the kidney. *Eur. J. Radiol.* 2010;76:337-347.

15. Katzberg RW, Buonocore MH, Ivanovic M, Pellot-Barakat C, Ryan JM, Whang K, Brock JM, Jones CD. Functional, dynamic, and anatomic MR urography: feasibility and preliminary findings. *Acad. Radiol.* 2001;8:1083-1099.

16. Egger C, Cannet C, Gerard C, Debon C, Stohler N, Dunbar A, Tigani B, Li J, Beckmann N. Adriamycin-induced nephropathy in rats: functional and cellular effects characterized by MRI. *J. Magn. Reson. Imaging.* 2015;41:829-840.

17. Hamm LL, Nakhoul N, Hering-Smith KS. Acid-Base Homeostasis. *Clin J Am Soc Nephrol.* 2015;10:2232-2242.

18. Hingorani DV, Bernstein AS, Pagel MD. A review of responsive MRI contrast agents: 2005-2014. *Contrast Media Mol. Imaging.* 2015;10:245-265.

19. Vinogradov E, Sherry AD, Lenkinski RE. CEST: from basic principles to applications, challenges and opportunities. *J. Magn. Reson.* 2013;229:155-172.

20. Liu G, Song X, Chan KW, McMahon MT. Nuts and bolts of chemical exchange saturation transfer MRI. *NMR Biomed.* 2013;26:810-828.

21. Longo DL, Dastru W, Digilio G, Keupp J, Langereis S, Lanzardo S, Prestigio S, Steinbach O, Terreno E, Uggeri F, Aime S. Iopamidol as a responsive MRI-chemical exchange saturation transfer contrast agent for pH mapping of kidneys: In vivo studies in mice at 7 T. *Magn. Reson. Med.* 2011;65:202-211.

22. McVicar N, Li AX, Suchy M, Hudson RH, Menon RS, Bartha R. Simultaneous in vivo pH and temperature mapping using a PARACEST-MRI contrast agent. *Magn. Reson. Med.* 2013;70:1016-1025.

23. Longo DL, Sun PZ, Consolino L, Michelotti FC, Uggeri F, Aime S. A general MRI-CEST ratiometric approach for pH imaging: demonstration of in vivo pH mapping with iobitridol. *J. Am. Chem. Soc.* 2014;136:14333-14336.

24. Moon BF, Jones KM, Chen LQ, Liu P, Randtke EA, Howison CM, Pagel MD. A comparison of iopromide and iopamidol, two acidoCEST MRI contrast media that measure tumor extracellular pH. *Contrast Media Mol. Imaging.* 2015;10:446-455.

25. Yang X, Song X, Ray Banerjee S, Li Y, Byun Y, Liu G, Bhujwalla ZM, Pomper MG, McMahon MT. Developing imidazoles as CEST MRI pH sensors. *Contrast Media Mol. Imaging.* 2016;11:304-312.

26. Wu Y, Zhang S, Soesbe TC, Yu J, Vinogradov E, Lenkinski RE, Sherry AD. pH imaging of mouse kidneys in vivo using a frequency-dependent paraCEST agent. *Magn. Reson. Med.* 2016;75:2432-2441.

27. Delli Castelli D, Ferrauto G, Cutrin JC, Terreno E, Aime S. In vivo maps of extracellular pH in murine melanoma by CEST-MRI. *Magn. Reson. Med.* 2014;71:326-332.

28. Longo DL, Bartoli A, Consolino L, Bardini P, Arena F, Schwaiger M, Aime S. In vivo imaging of tumour metabolism and acidosis by combining PET and MRI-CEST pH imaging. *Cancer Res.* 2016. doi:10.1158/0008-5472.CAN-16-0825

29. Muller-Lutz A, Khalil N, Schmitt B, Jellus V, Pentang G, Oeltzschner G, Antoch G, Lanzman RS, Wittsack HJ. Pilot study of Iopamidol-based quantitative pH imaging on a clinical 3T MR scanner. *MAGMA.* 2014;27:477-485.

30. Longo DL, Busato A, Lanzardo S, Antico F, Aime S. Imaging the pH evolution of an acute kidney injury model by means of iopamidol, a MRI-CEST pH-responsive contrast agent. *Magn. Reson. Med.* 2013;70:859-864.

31. Le Clef N, Verhulst A, D'Haese PC, Vervaet BA. Unilateral Renal Ischemia-Reperfusion as a Robust Model for Acute to Chronic Kidney Injury in Mice. *PLoS One.* 2016;11:e0152153.

32. Chiazza F, Chegaev K, Rogazzo M, Cutrin JC, Benetti E, Lazzarato L, Fruttero R, Collino M. A nitric oxide-donor furoxan moiety improves the efficacy of edaravone against early renal dysfunction and injury evoked by ischemia/reperfusion. *Oxid Med Cell Longev.* 2015;2015:804659.

33. Mehta RL, Kellum JA, Shah SV, Molitoris BA, Ronco C, Warnock DG, Levin A. Acute Kidney Injury Network: report of an initiative to improve outcomes in acute kidney injury. *Crit Care.* 2007;11:R31.

34. Wei Q, Dong Z. Mouse model of ischemic acute kidney injury: technical notes and tricks. *Am J Physiol Renal Physiol.* 2012;303:F1487-1494.

35. Vogt MT, Farber E. On the molecular pathology of ischemic renal cell death. Reversible and irreversible cellular and mitochondrial metabolic alterations. *Am. J. Pathol.* 1968;53:1-26.

36. Dujardin M, Sourbron S, Luypaert R, Verbeelen D, Stadnik T. Quantification of renal perfusion and function on a voxel-by-voxel basis: a feasibility study. *Magn. Reson. Med.* 2005;54:841-849.

37. Sourbron SP, Michaely HJ, Reiser MF, Schoenberg SO. MRI-measurement of perfusion and glomerular filtration in the human kidney with a separable compartment model. *Invest. Radiol.* 2008;43:40-48.

38. Zollner FG, Schock-Kusch D, Backer S, Neudecker S, Gretz N, Schad LR. Simultaneous measurement of kidney function by dynamic contrast enhanced MRI and FITC-sinistrin clearance in rats at 3 tesla: initial results. *PLoS One.* 2013;8:e79992.

39. Buonocore MH, Katzberg RW. Estimation of extraction fraction (EF) and glomerular filtration rate (GFR) using MRI: considerations derived from a new Gd-chelate biodistribution model simulation. *IEEE Trans. Med. Imaging.* 2005;24:651-666.

40. Zhang JL, Rusinek H, Chandarana H, Lee VS. Functional MRI of the kidneys. *J. Magn. Reson. Imaging.* 2013;37:282-293.

41. Longo DL, Michelotti F, Consolino L, Bardini P, Digilio G, Xiao G, Sun PZ, Aime S. In Vitro and In Vivo Assessment of Nonionic Iodinated Radiographic Molecules as Chemical Exchange Saturation Transfer Magnetic Resonance Imaging Tumor Perfusion Agents. *Invest. Radiol.* 2016;51:155-162.

42. Anemone A, Consolino L, Longo DL. MRI-CEST assessment of tumour perfusion using X-ray iodinated agents: comparison with a conventional Gd-based agent. *Eur. Radiol.* 2016. doi:10.1007/s00330-016-4552-7

43. Kovesdy CP, Anderson JE, Kalantar-Zadeh K. Association of serum bicarbonate levels with mortality in patients with non-dialysis-dependent CKD. *Nephrol. Dial. Transplant.* 2009;24:1232-1237.

44. Sise ME, Courtwright AM, Channick RN. Pulmonary hypertension in patients with chronic and end-stage kidney disease. *Kidney Int.* 2013;84:682-692.

45. Dixon WT, Hancu I, Ratnakar SJ, Sherry AD, Lenkinski RE, Alsop DC. A multislice gradient echo pulse sequence for CEST imaging. *Magn. Reson. Med.* 2010;63:253-256.

46. Sun PZ, Cheung JS, Wang E, Benner T, Sorensen AG. Fast multislice pH-weighted chemical exchange saturation transfer (CEST) MRI with Unevenly segmented RF irradiation. *Magn. Reson. Med.* 2011;65:588-594.

Figure legends

Figure 1. Renal histological features. (A) Histopathological damage score was assessed at baseline, and at 1 and 7 days after moderate (20 min) and severe (40 min) ischemia/reperfusion injury in mice. (B) Representative images of the outer external medulla region from H&E stained kidney sections of sham and after moderate or severe ischemia reperfusion injury. (Magnification 200x).

Figure 2. Clinical biomarkers of ischemia-reperfusion injury. Clinical biomarker levels of (A) serum creatinine, (B) blood urea nitrogen and (C) urinary pH values for sham and renal ischemia-reperfusion injured mice were assessed at baseline, and at 1 and 7 days after moderate (20 min) and severe (40 min) ischemia/reperfusion injury in mice.

Figure 3. MRI-CEST pH assessment of ischemia-reperfusion injury and evolution. (A) Bar graph showing renal pH values in clamped and contralateral kidneys before and after moderate ischemia (20 min) reperfusion injury at several time points. (B) Bar graph showing renal pH values in clamped and contralateral kidneys before and after severe ischemia (40 min) reperfusion injury at several time points. (C) Correlation of histological score and MRI-CEST based pH values in mice imaged after moderate and severe ischemia reperfusion injury at day 0, day 1 and day 7. Significant differences compared with the contralateral kidney without AKI at the same time point and with baseline (PRE) are indicated as */*, respectively. * = $P<0.05$, ** = $P<0.01$.

Figure 4. MRI-CEST pH mapping detects renal pH changes and regional distribution of damage after moderate and severe unilateral AKI. (A,C) Representative T_2-weighted anatomical images before and after moderate (A) and severe (C) AKI at different time points (day 1, day 2 and day 7) showing clamped (right) and contralateral normal kidney (left). (B,D) Representative MRI-CEST pH maps overimposed onto anatomical images before and after moderate (B) and severe (D) AKI at different time points (day 1, day 2 and day 7) showing pronounced alkalinazation and reduced filtration (not coloured pixels within the renal region) of the pH-responsive contrast agent in clamped kidney in comparison to contralateral kidney.

Figure 5. MRI-CEST filtration fraction assessment of ischemia reperfusion injury and evolution. (A) Bar graph showing filtration fraction values in clamped and contralateral kidneys before and after moderate ischemia (20 min) reperfusion injury at several time points. (B) Bar graph showing renal filtration fraction values in clamped and contralateral kidneys before and after severe ischemia (40 min) reperfusion injury at several time points. Significant differences compared with the contralateral kidney without AKI at the same time point and with baseline (PRE) are indicated as */*, respectively. * = $P<0.05$, ** = $P<0.01$, *** = $P<0.001$.

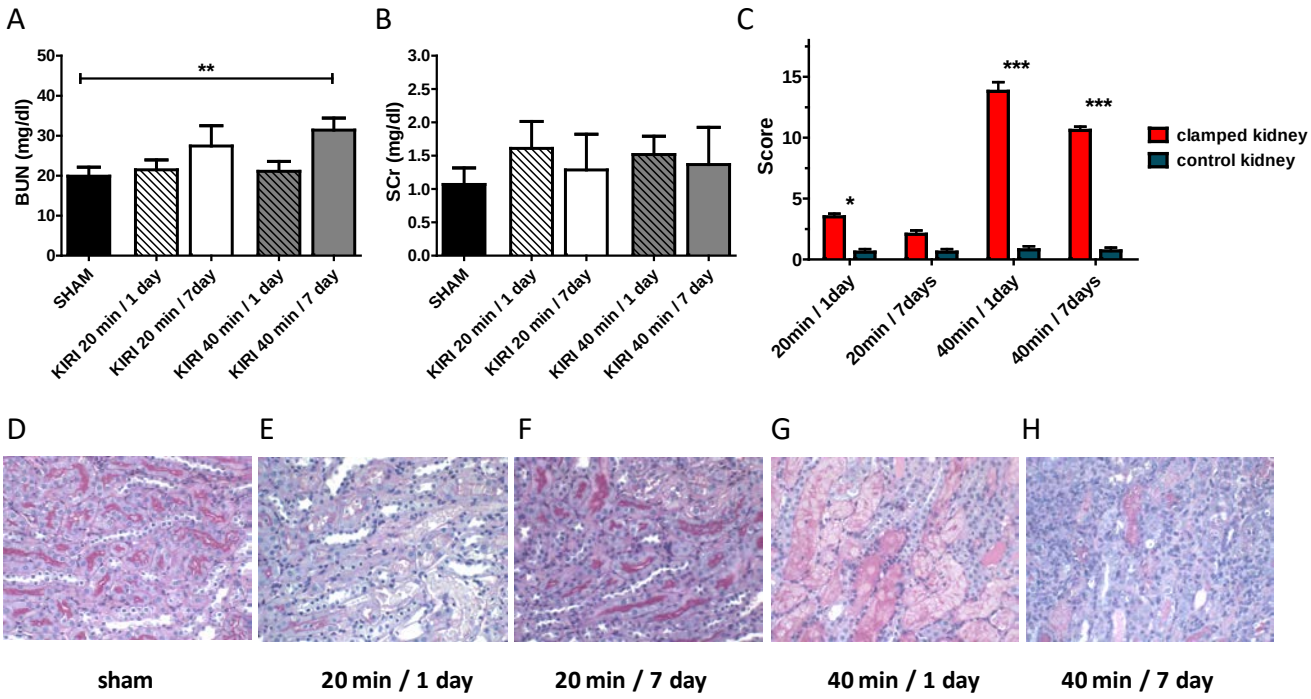
A
B
C
BUN (mg/dl)
SCr (mg/dl)
Score
**
*
***
***
SHAM
KIRI 20 min / 1 day
KIRI 20 min / 7day
KIRI 40 min / 1 day
KIRI 40 min / 7 day
20min / 1day
20min / 7days
40min / 1day
40min / 7days
clamped kidney
control kidney
D
E
F
G
H
sham
20 min / 1 day
20 min / 7 day
40 min / 1 day
40 min / 7 day

Figure 1

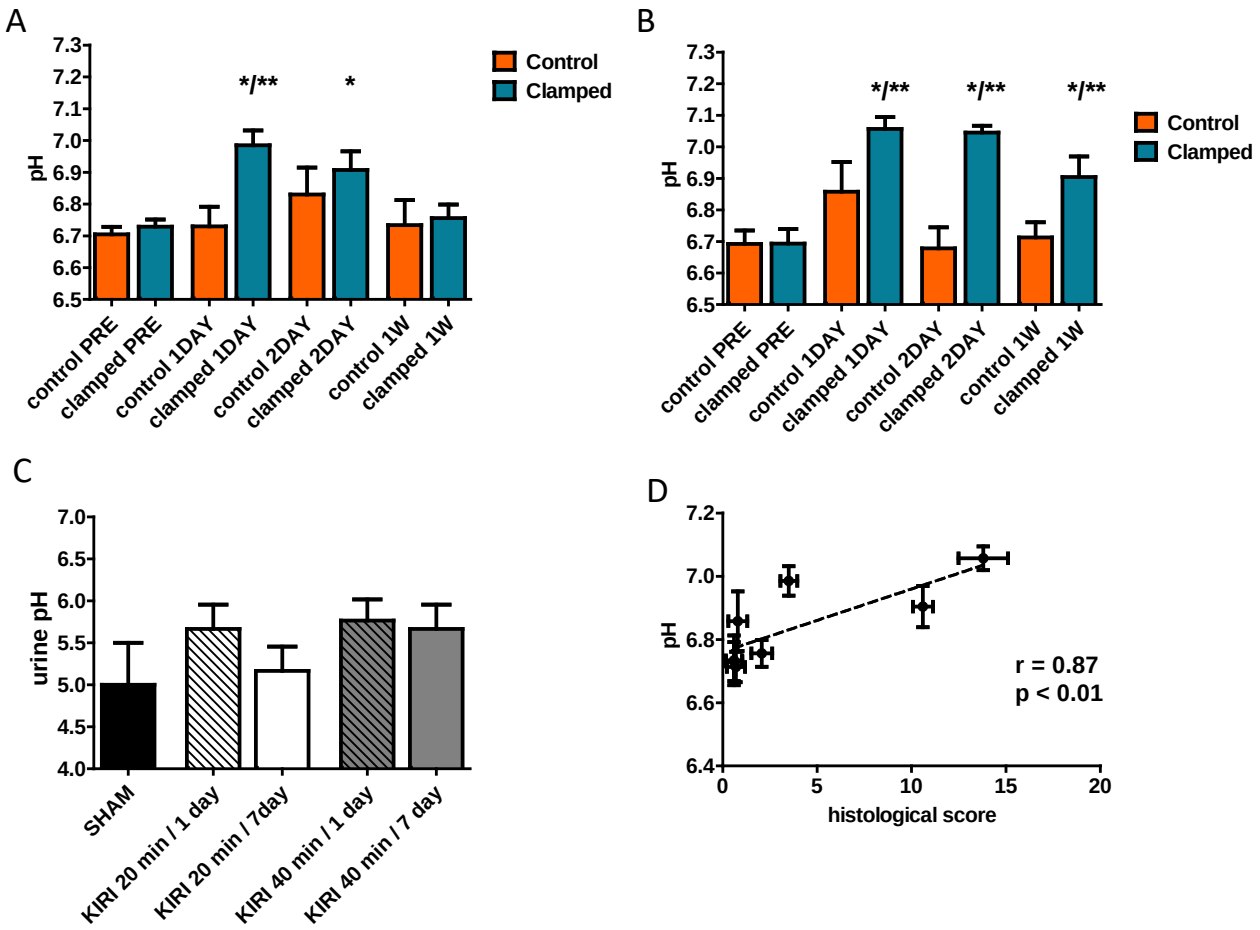
A
pH
7.3
7.2
7.1
7.0
6.9
6.8
6.7
6.6
6.5
*/**
*
Control
Clamped
control PRE
clamped PRE
control 1DAY
clamped 1DAY
control 2DAY
clamped 2DAY
control 1W
clamped 1W
B
pH
*/**
*/**
*/**
Control
Clamped
control PRE
clamped PRE
control 1DAY
clamped 1DAY
control 2DAY
clamped 2DAY
control 1W
clamped 1W
C
urine pH
7.0
6.5
6.0
5.5
5.0
4.5
4.0
SHAM
KIRI 20 min / 1 day
KIRI 20 min / 7day
KIRI 40 min / 1 day
KIRI 40 min / 7 day
D
pH
7.2
7.0
6.8
6.6
6.4
0
5
10
15
20
histological score
r = 0.87
p < 0.01

Figure 2

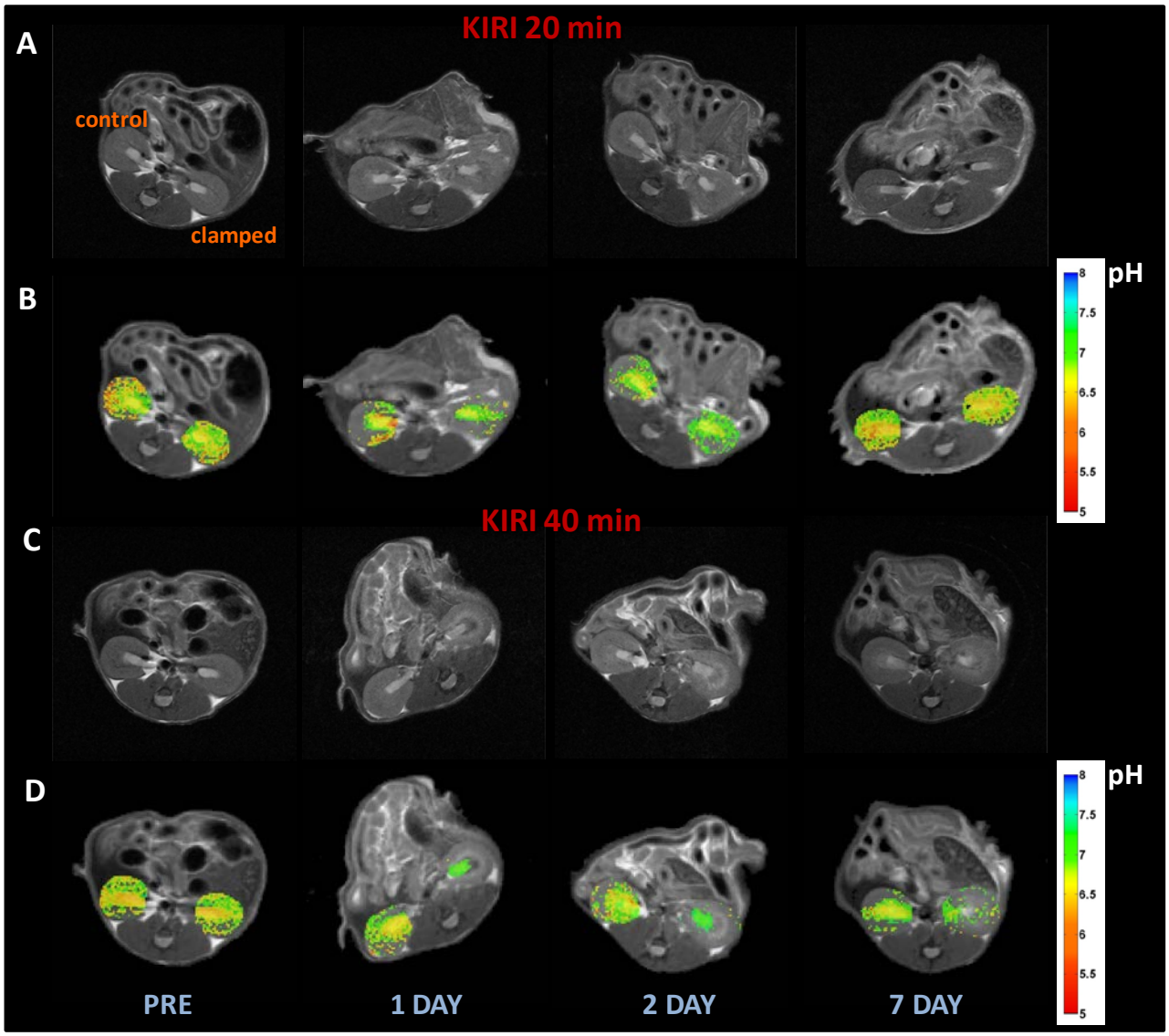
A
KIRI 20 min
control
clamped
B
pH
8
7.5
7
6.5
6
5.5
5
C
KIRI 40 min
D
pH
8
7.5
7
6.5
6
5.5
5
PRE
1 DAY
2 DAY
7 DAY

Figure 3

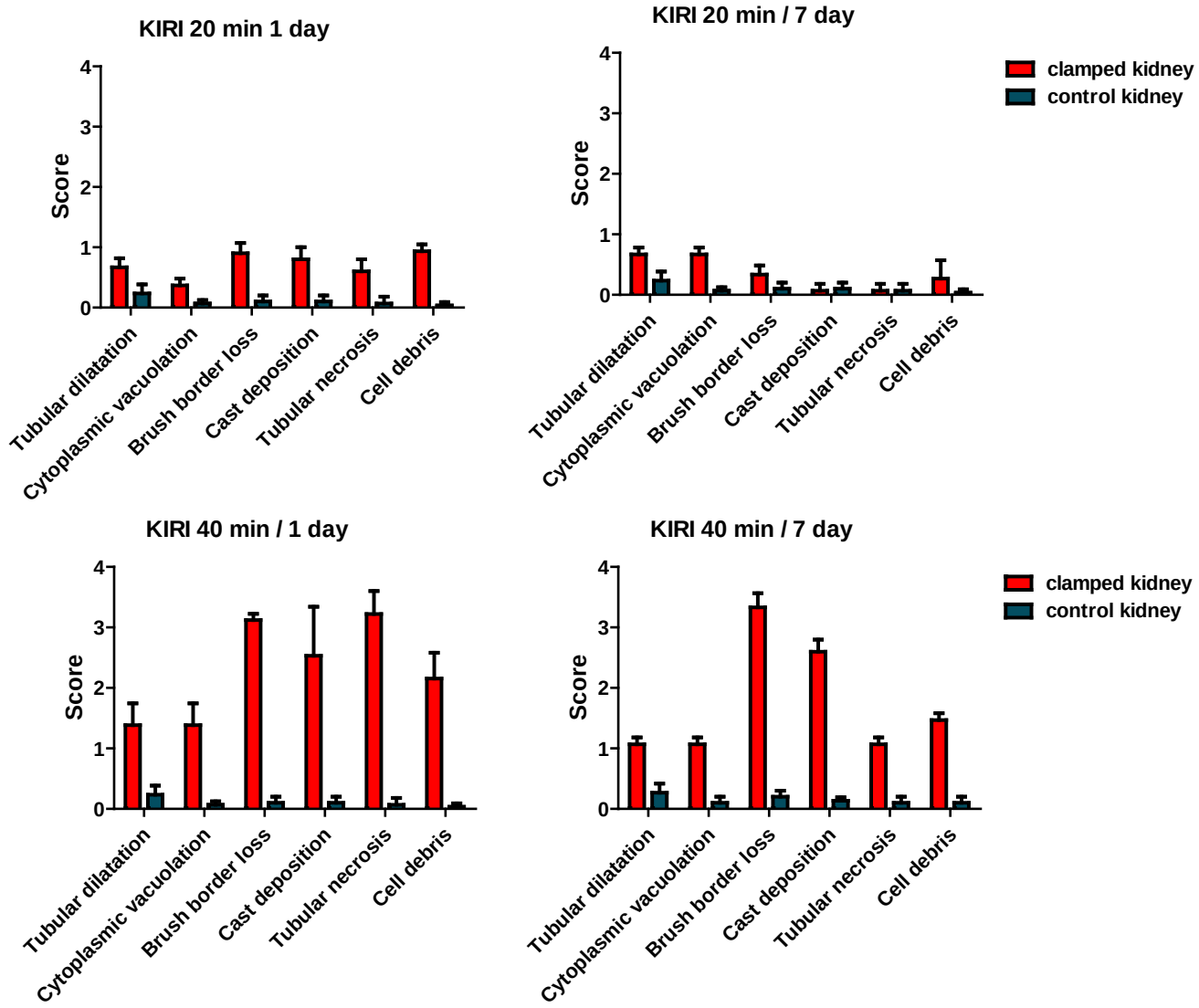

Figure S1. Average histological scores of renal damage. Clamped and control kidneys are indicated in red and blue, respectively. Values are presented as the mean ±standard deviations.

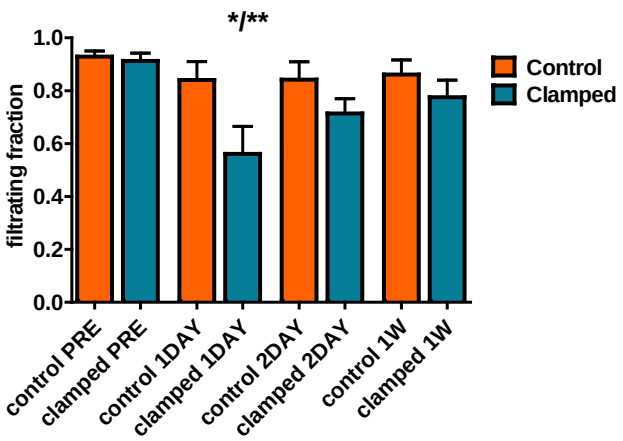
*/**
filtrating fraction
1.0
0.8
0.6
0.4
0.2
0.0
Control
Clamped
control PRE
clamped PRE
control 1DAY
clamped 1DAY
control 2DAY
clamped 2DAY
control 1W
clamped 1W

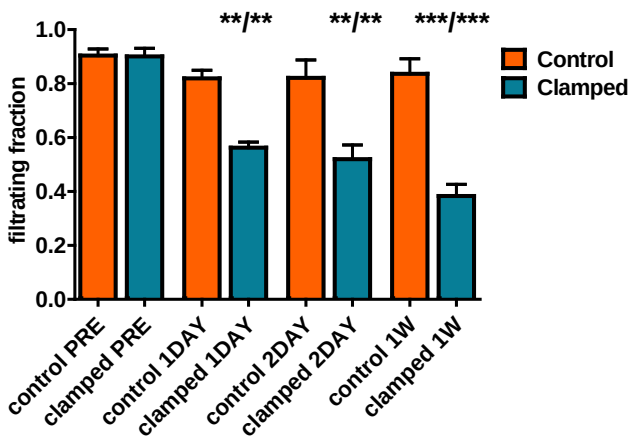
/
/
/
filtrating fraction
1.0
0.8
0.6
0.4
0.2
0.0
Control
Clamped
control PRE
clamped PRE
control 1DAY
clamped 1DAY
control 2DAY
clamped 2DAY
control 1W
clamped 1W